

***New Phytologist* Supporting Information**

Article title: The immune repressor *BIR1* contributes to antiviral defense and undergoes transcriptional and post-transcriptional regulation during viral infections

Authors: Irene Guzmán-Benito, Livia Donaire, Vítor Amorim-Silva, José G. Vallarino, Alicia Esteban, Andrzej T. Wierzbicki, Virginia Ruíz-Ferrer, César Llave

Article acceptance date: 15 May 2019

The following Supporting Information is available for this article:

SUPPORTING INFORMATION

Figure S1. Effect of RNA silencing on *BIR1* expression in plants infected with TuMV.

Figure S2. Epigenetic regulation of *BIR1* and RdDM-methylation controls.

Figure S3. Methylation status of the *BIR1* promoter using whole-genome bisulfite sequencing (WGBS) data in Arabidopsis.

Figure S4. Methylation status of the *BIR1* promoter using in-house bisulfite sequencing in Arabidopsis.

Figure S5. Epigenetic regulation of *BIR1* and RdDM-methylation controls in salicylic acid (SA)-treated plants.

Figure S6. *BIR1* mRNA accumulation in RNA silencing mutants, cleavage mapping at the 5' UTR of *BIR1* mRNA and viral accumulation in *N. benthamiana* leaves expressing *BIR1*.

Figure S7. DEX-inducible system for overexpression of *BIR1* in Arabidopsis plants.

Figure S8. Phenotypes of *BIR1* overexpressing transgenic Arabidopsis.

Figure S9. Phenotypes of *BIR1* overexpressing transgenic seedlings grown in axenic conditions.

Figure S10. Model of *BIR1* regulation

Table S1. List of primers.

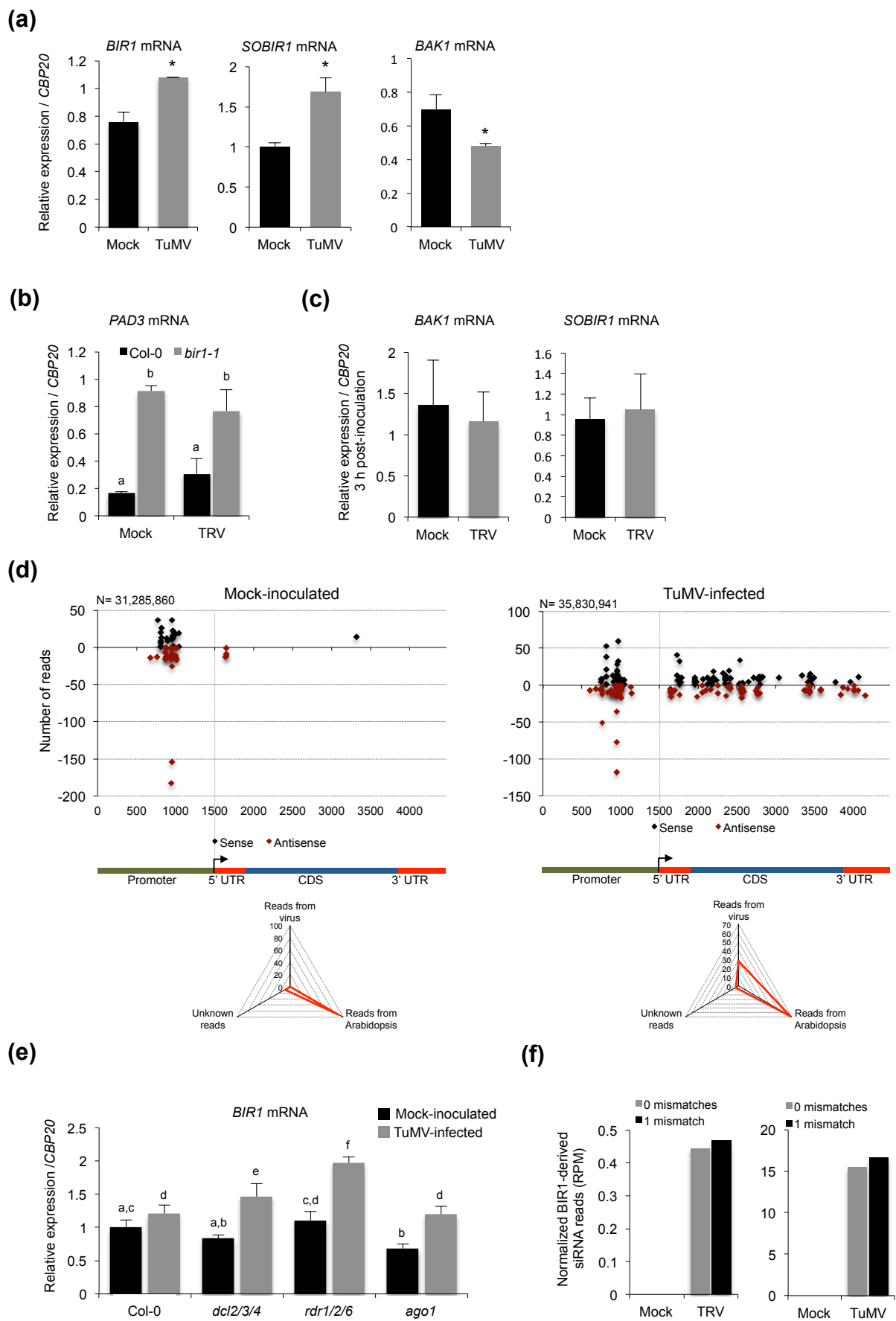


Fig. S1

Figure S1. Effect of RNA silencing on *BIR1* expression in plants infected with TuMV. **(a)** Accumulation of *BIR1*, *SOBIR1* and *BAK1* transcripts in leaves of mock-inoculated and TuMV-infected plants at 10 days post-inoculation (dpi). **(b)** Accumulation of defense-related *PAD3* transcripts in mock-inoculated or TRV-infected leaves of Arabidopsis wild type (Col-0) and *bir1-1* mutants at 8 dpi. **(c)** Accumulation of *BAK1* and *SOBIR1* transcripts in leaves of mock-inoculated and TRV-infected plants at 3 hours post-inoculation. **(d)** Distribution of *BIR1*-derived siRNAs in rosette leaves of mock-inoculated and TuMV-infected Arabidopsis plants. Sense (black dots) and antisense (red dots) siRNA species are represented as positive and negative values in the Y-axis, respectively. The triangle graph represents the genomic distribution (percentage) of sRNAs in the sequenced set. N denotes the total number of filtered sequenced reads. **(e)** Accumulation of *BIR1* transcripts in rosette leaves from mock-inoculated and TuMV-infected plants of Arabidopsis wild type and RNA silencing mutants [*dcl2 dcl3 dcl4 (dcl2/3/4)*, *rdr1 rdr2 rdr6 (rdr1/2/6)* and *ago1*]. **(f)** Comparative accumulation of *BIR1*-derived siRNAs determined by deep sequencing analysis between mock-inoculated plants and plants infected with TRV (left) or TuMV (right). Results from sequence alignments using 0 or 1 mismatch are shown. Relative expression levels were determined by qRT-PCR and normalized to the *CBP20* internal control. Error bars represent SD from three independent PCR measurements. Asterisks (Student's *t* test) or different letters (one-way ANOVA) were used to indicate significant differences ($P < 0.001$). The experiments of gene expression were repeated at least three times with similar results and one representative biological replicate is shown.

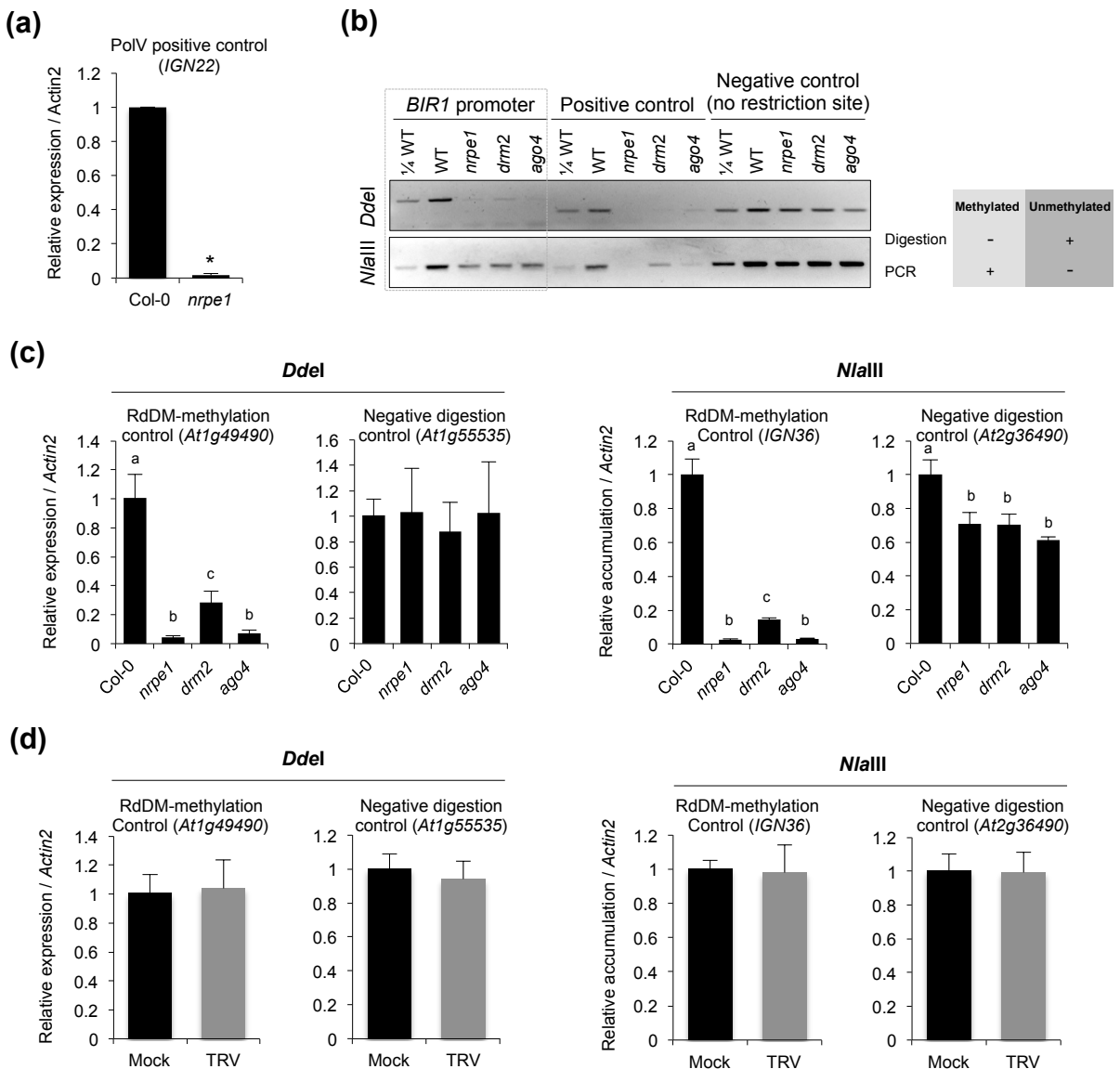


Figure S2. Epigenetic regulation of *BIR1* and RdDM-methylation controls. **(a)** Accumulation of Pol V-dependent *IGN22* transcripts (Pol V positive control) in rosette leaves of wild type (Col-0) and *nrpe1* mutants. **(b)** Chop-PCR with genomic DNA isolated from rosette leaves of wild type (WT) and RdDM mutants (*nrpe1*, *drm2* and *ago4*). The DNA was digested with methylation-sensitive enzymes *DdeI* and *NlaIII* and a region of ~400 nts within the *BIR1* promoter was PCR amplified using flanking primers. The RdDM targets *At1g49490* and *IGN36* were used as positive controls for *DdeI* and *NlaIII* digestions, respectively. Regions lacking a restriction site were used as negative control. **(c)** Extent of asymmetric cytosine methylation of RdDM controls in rosette leaves of wild type and RdDM mutants [*nrpe1*, *drm2* and *ago4*] determined by chop-qPCR. *At1g49490* and *IGN36* were used as RdDM-methylation controls for *DdeI* and *NlaIII* digestions, respectively. Regions lacking a restriction site (*At1g55535* and *At2g36490*) were used as negative digestion controls. **(d)** Extent of asymmetric cytosine methylation of RdDM controls in rosette leaves of mock-inoculated and TRV-infected plants determined by chop-qPCR at 8 days post-inoculation (dpi). *At1g49490* and *IGN36* were used as RdDM-methylation controls for *DdeI* and *NlaIII* digestions, respectively. Regions lacking a restriction site (*At1g55535* and *At2g36490*) were used as negative digestion controls. Relative expression levels were determined by qRT-PCR or qPCR and normalized to the *CBP20* or *Actin2* internal control as indicated. Error bars in (a) represent SD from three independent PCR measurements. Values in (c) and (d) are means \pm SD from at least three independent biological replicates. Asterisks (Student's *t* test) or different letters (one-way ANOVA) were used to indicate significant differences ($P < 0.001$). The experiments were repeated at least three times with similar results and one representative biological replicate is shown.

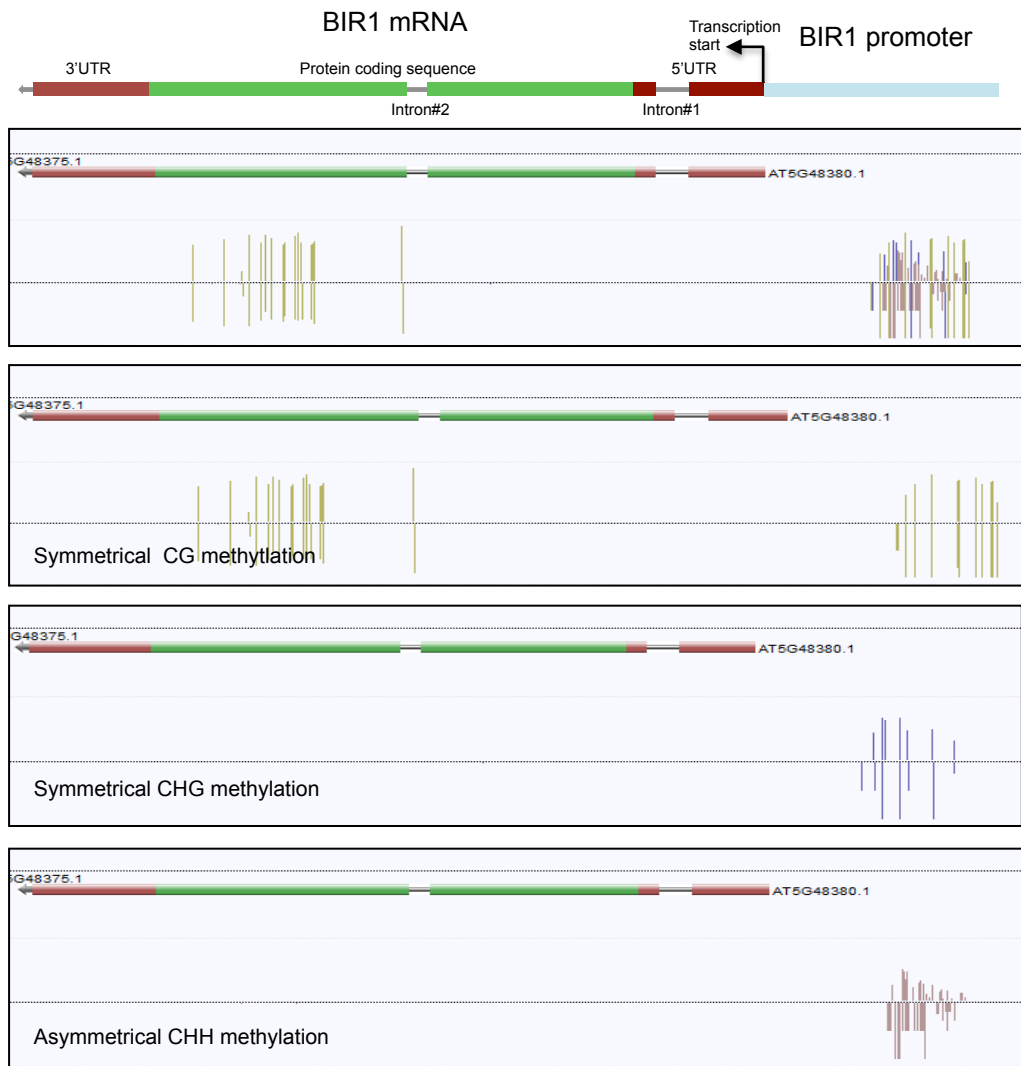


Figure S3. Methylation status of the *BIR1* promoter using whole-genome bisulfite sequencing (WGBS) data in Arabidopsis. The Genome browser screenshot shows the distribution of symmetrical (CG and CHG) and asymmetrical (CHH) methylation at the *BIR1* locus (Stroud *et al.*, 2013). The *BIR1* gene is schematically represented (red, 5' and 3' untranslated regions; green, exons; grey bars, introns; light blue, promoter). The arrow indicates the transcription start site. Methylation is mostly located upstream of the *BIR1* transcription initiation site.

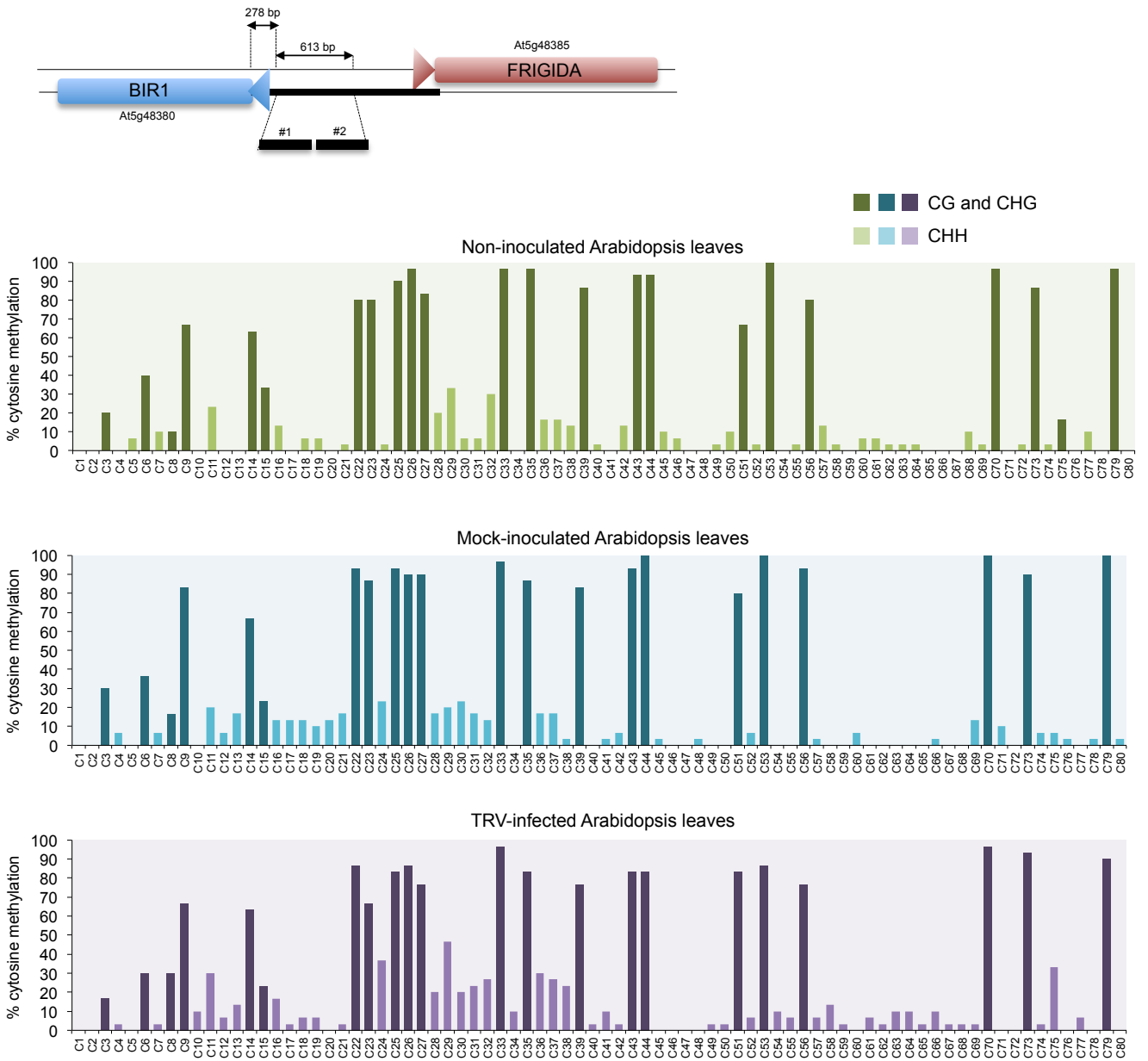
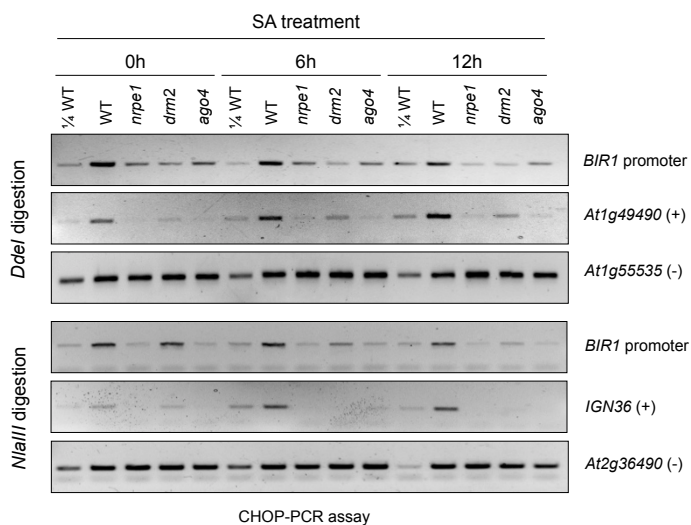
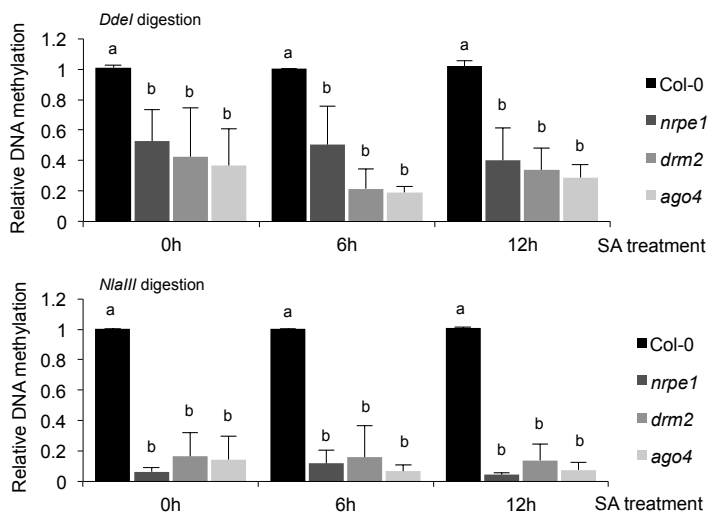


Figure S4. Methylation status of the *BIR1* promoter using in-house bisulfite sequencing in Arabidopsis. Graphic representation of the genomic regions (#1 and #2) analyzed. Comparison of cytosine methylation at symmetric (CG and CHG) and asymmetric (CHH) sites within the *BIR1* promoter between non-inoculated, mock-inoculated and TRV-infected leaves at 8 days post-inoculation (dpi). Percentages of methylcytosines at each genomic position are given.

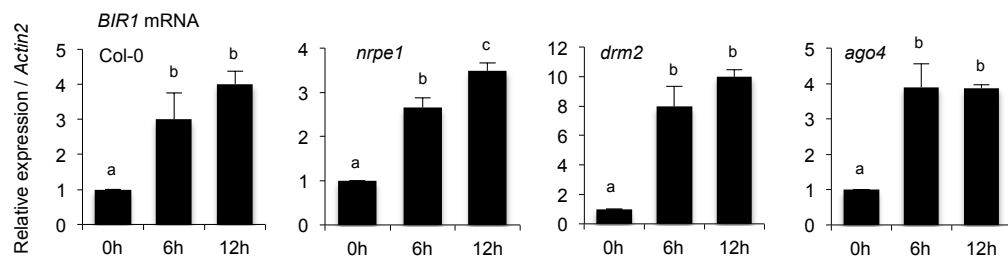
(a)



(b)



(c)



(d)

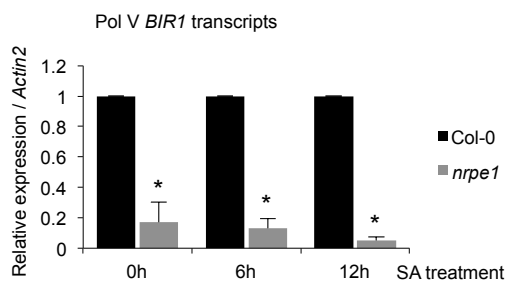
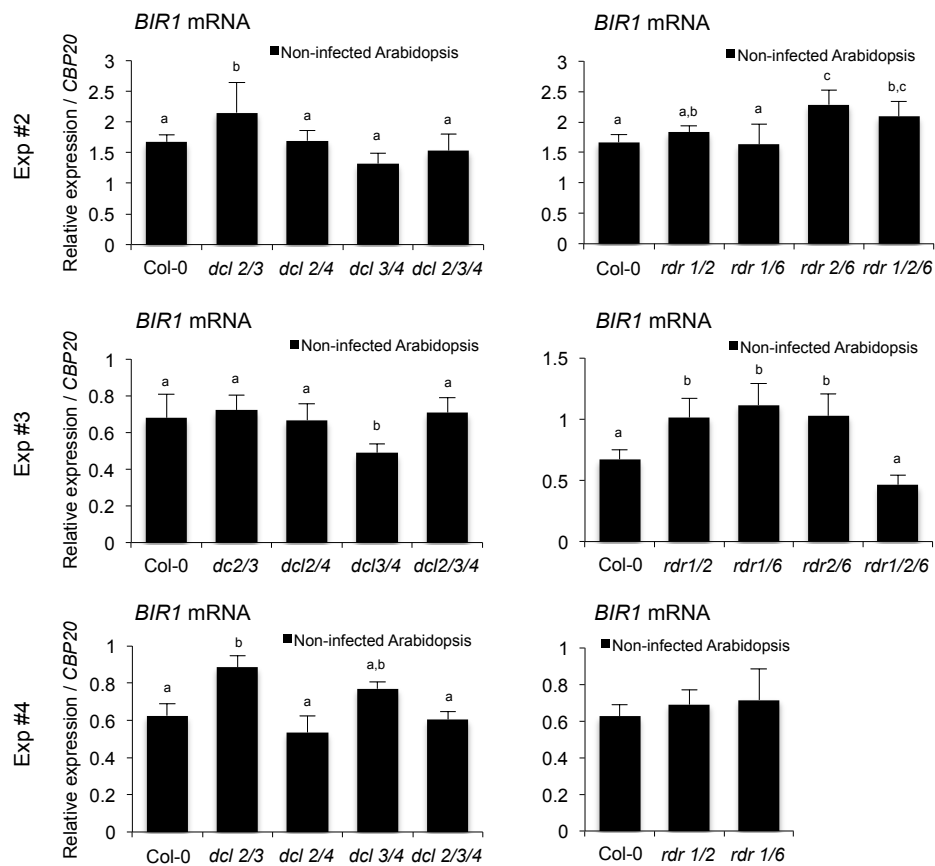


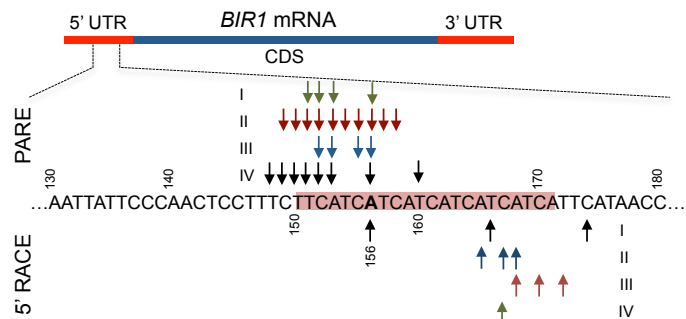
Fig. S5

Figure S5. Epigenetic regulation of *BIR1* and RdDM-methylation controls in salicylic acid (SA)-treated plants. **(a)** Chop-PCR with genomic DNA isolated from rosette leaves of wild type (WT) and RdDM mutants (*nrpe1*, *drm2* and *ago4*) at 0, 6 and 12 h after SA treatment. The DNA was digested with methylation-sensitive enzymes and a region of ~400 nts within the *BIR1* promoter was PCR amplified using flanking primers. The RdDM targets *At1g49490* and *IGN36* were used as positive controls for *DdeI* and *NlaIII* digestions, respectively. Regions lacking a restriction site (*At1g55535* and *At2g36490*) were used as negative digestion controls. **(b)** Extent of asymmetric cytosine methylation at the *BIR1* promoter in rosette leaves of wild type (Col-0) and RdDM mutants (*nrpe1*, *drm2* and *ago4*) determined by chop-qPCR at 0, 6 and 12 h after SA treatment. **(c)** Accumulation of *BIR1* transcripts in rosette leaves of wild type and RdDM mutants (*nrpe1*, *drm2* and *ago4*) at 0, 6 and 12 h after SA treatment. **(d)** Accumulation of Pol V-dependent *BIR1* transcripts in rosette leaves of wild type and *nrpe1* mutants at 0, 6 and 12 h after SA treatment. Relative expression levels were determined by qRT-PCR or qPCR and normalized to the *Actin2* internal control. Values in (b) and (c) are means \pm SD from at least three independent biological replicates. Error bars in (d) represent SD from three independent PCR measurements. Experiments in (d) were repeated twice with similar results and one representative biological replicate is shown. Asterisks (Student's *t* test) or different letters (one-way ANOVA) were used to indicate significant differences ($P < 0.001$).

(a)



(b)



(c)

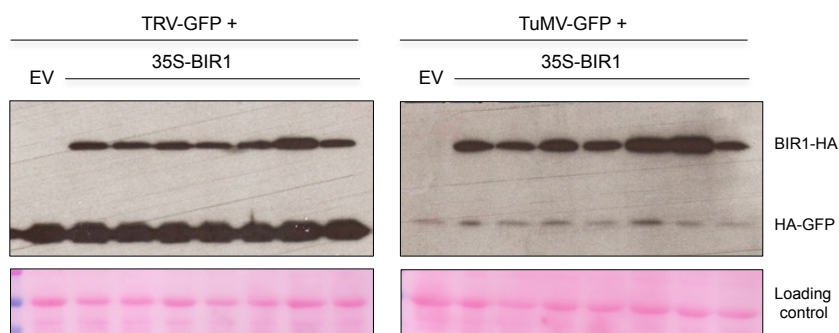


Fig. S6

Figure S6. *BIR1* mRNA accumulation in RNA silencing mutants, cleavage mapping at the 5' UTR of *BIR1* mRNA and viral accumulation in *N. benthamiana* leaves expressing *BIR1* **(a)** Accumulation of *BIR1* transcripts in non-infected rosette leaves of wild type (Col-0) and mutants impaired in siRNA biogenesis [*dcl2 dcl3* (*dcl2/3*), *dcl2 dcl4* (*dcl2/4*), *dcl3 dcl4* (*dcl3/4*) or *dcl2 dcl3 dcl4* (*dcl2/3/4*)] and secondary siRNA biogenesis [*rdr1 rdr2* (*rdr1/2*), *rdr2 rdr6* (*rdr2/6*), *rdr1 rdr6* (*rdr1/6*) or *rdr1 rdr2 rdr6* (*rdr1/2/6*)]. Results from three independent replicates (Exp #2, Exp#3 and Exp 4) are shown. Data from Exp #1 are shown in Fig. 5. Relative expression levels were determined by qRT-PCR and normalized to the *CBP20* internal control. Error bars represent SD from three independent PCR measurements. Different letters indicate significant differences according to one-way ANOVA and Duncan test ($P < 0.001$). **(b)** Analysis of cDNA ends was done by PARE sequencing of 5' degradome signatures (top) and conventional 5' RACE (bottom). Degradome libraries: I, mock-inoculated leaves (14 days post-inoculation); II, TuMV-infected leaves (14 dpi); III, TRV-infected leaves (8 dpi); IV, mock-inoculated leaves (8 dpi). **(c)** Western blot analysis of *BIR1* and GFP proteins in extracts from leaves co-infiltrated with *BIR1*-HA constructs in the presence of an infectious TRV-GFP (left) or TuMV-GFP (right) recombinant clone. GFP protein levels were used to infer the relative viral accumulation. Ponceau staining was used as a protein loading control. The experiments in (a) and (c) were repeated four times and one representative biological replicate is shown.

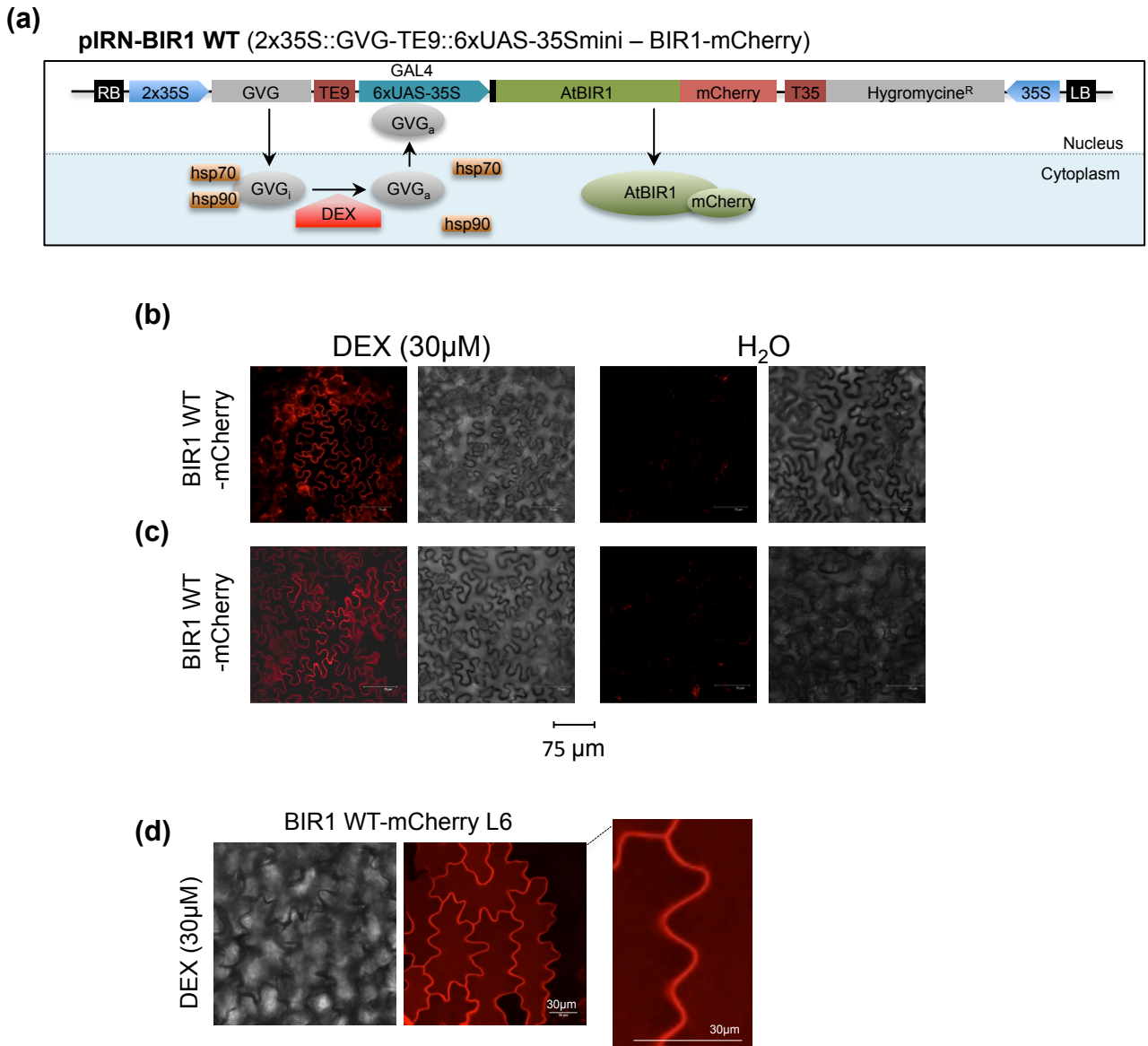
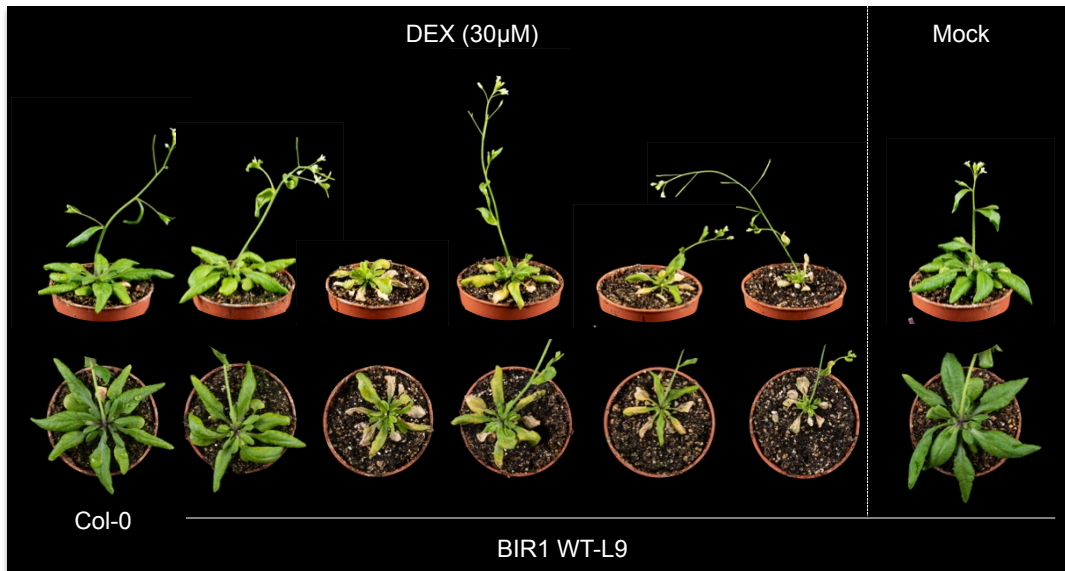
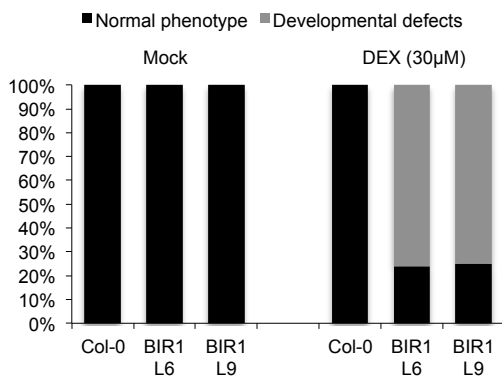


Figure S7. DEX-inducible system for overexpression of *BIR1* in Arabidopsis plants. **(a)** Schematic representation of the glucocorticoid (DEX)-inducible system used for conditional *BIR1* expression in stably transformed Arabidopsis plants. Detailed description is provided by (McNellis *et al.*, 1998). **(b)** and **(c)** Visualization of the distribution of fluorescence derived from mCherry protein-tagged BIR1 constructs. Constructs were introduced by agroinfiltration in *N. benthamiana* leaves, followed by Confocal Microscopy of epidermal cells at 2 days post-inoculation (dpi). Samples were treated with 30 μ M DEX or water as indicated. DEX was sprayed on the leaf surface (b) or agroinjected on the spot (c). Bar, 75 μ m. **(d)** Visualization of the distribution of fluorescence derived from the mCherry protein-tagged BIR1 coding transgene in Arabidopsis. Samples were collected from young seedlings grown on MS plates, and analyzed by Confocal Microscopy of epidermal cells. Bar, 30 μ m. Plant tissue was imaged using a Leica TCS SP5 inverted confocal microscope with an Argon ion laser. mCherry was excited at 561 nm.

(a)



(b)



(c)

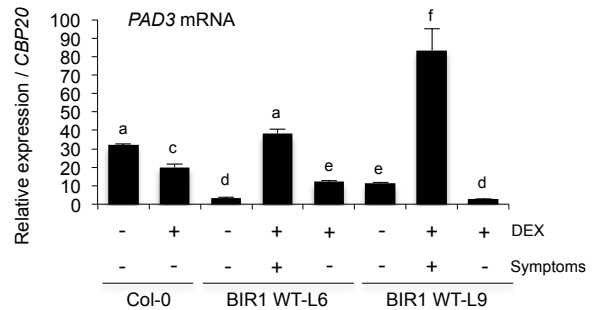
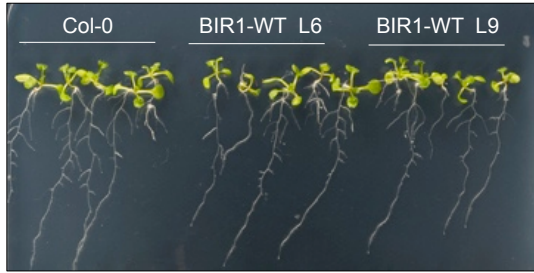
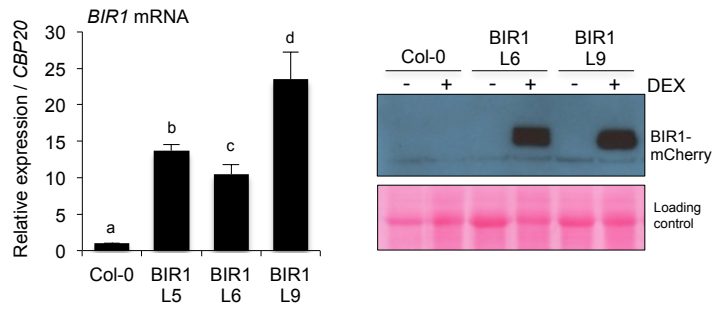


Figure S8. Phenotypes of *BIR1* overexpressing transgenic Arabidopsis. **(a)** Morphological phenotypes of *BIR1* transgenic plants after DEX treatment. Arabidopsis plants from transgenic line 9 (BIR1 WT L9) were grown for three weeks on soil and treated with 30 μ M DEX or mock-treated for 6 consecutive days by spraying the solution (1 ml per plant) once at 24h intervals. DEX-treated wild type (Col-0) plants are shown as controls. Plants were photographed at 7 days after the first DEX application. **(b)** Percentage of plants from wild type and transgenic *BIR1* overexpressing lines (L6 and L9) displaying normal vs morphological phenotypes after DEX treatments. Mock-inoculated plants are shown were used as controls. **(c)** Accumulation of defense-related *PAD3* transcripts in plants from lines L6 and L9. Wild-type plants are shown as controls. Plants were sprayed with DEX (+) or water (-). Plants showing wild type (-) or aberrant (+) phenotypes were analyzed. Relative expression levels were determined by qRT-PCR and normalized to the *CBP20* internal control. Error bars represent SD from three independent PCR measurements. Different letters indicate significant differences according to one-way ANOVA and Duncan test ($P < 0.001$). The experiments were repeated at least twice with similar results and one representative biological replicate is shown.

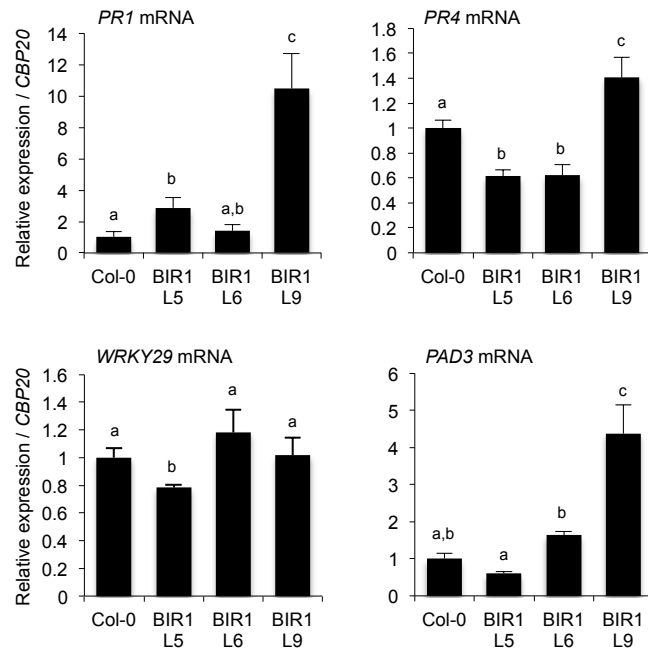
(a)



(b)



(c)



(d)

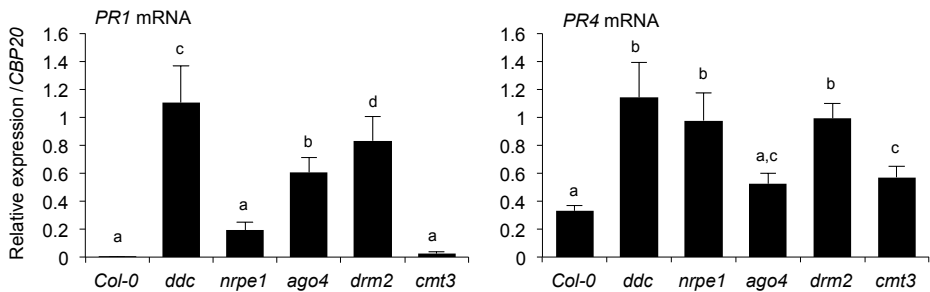


Fig. S9

Figure S9. Phenotypes of *BIR1* overexpressing transgenic seedlings grown in axenic conditions. **(a)** Growth phenotypes of plants from wild type (Col-0) and *BIR1* overexpressing lines (L6 and L9) grown under axenic conditions. **(b)** Accumulation of *BIR1* transcripts (left) and Western blot analysis of BIR1 protein (right) in seedlings of wild type and *BIR1* overexpressor lines (L5, L6 and L9). Water-treated plants (-) were used as controls. Ponceau staining was used as a protein loading control. **(c)** Accumulation of defense-related *PR1*, *PR4*, *PAD3* and *WRKY29* transcripts in samples used in (b). **(d)** Accumulation of *PR1* and *PR4* transcripts in rosette leaves of wild type and RdDM mutants (*cmt3*, *drm2*, *ddc*, *nrpe1* and *ago4*). Seedlings were grown on MS media containing 30 μ M DEX and samples were collected ten days after germination. Relative expression levels were determined by qRT-PCR and normalized to the *CBP20* internal control. Error bars represent SD from three independent PCR measurements. Different letters indicate significant differences according to one-way ANOVA and Duncan test ($P < 0.001$). The experiments were repeated at least three times with similar results and one representative biological replicate is shown.

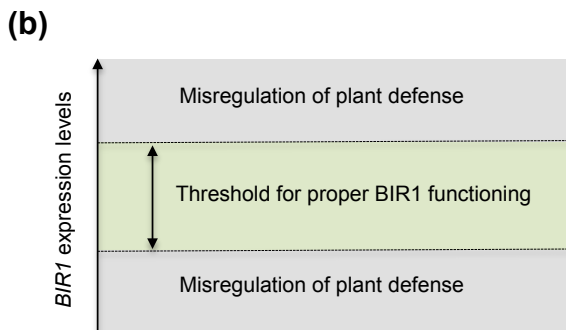
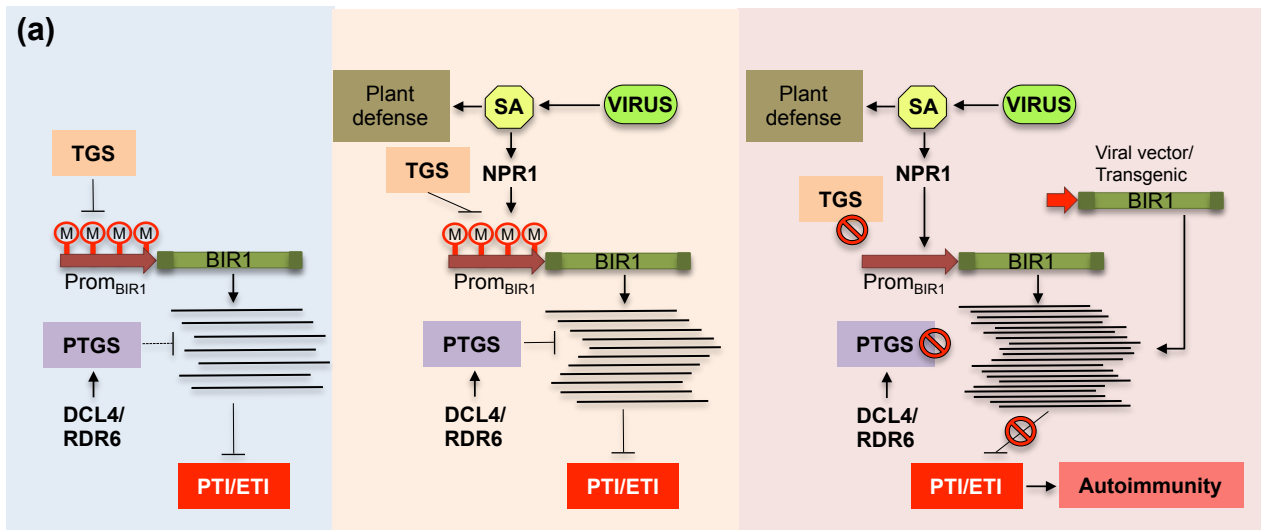


Figure S10. Model of *BIR1* regulation. **(a)** Transcriptional gene silencing (TGS) and post-transcriptional RNA silencing (PTGS) cooperate, alone or in conjunction with other mechanisms, to regulate *BIR1* expression levels both in the absence of pathogens and in virus-infected plants. Plant viruses promote salicylic acid (SA) accumulation that activates NPR1-dependent expression of *BIR1* as well as other SA-mediated defense responses. Disruption of RNA silencing (TGS and PTGS) or inducible/exogenous expression of a *BIR1* transgene leads to increasing levels of BIR1 in the plant tissue that may eventually affect proper BIR1 functioning and cause autoimmune phenotypes. **(b)** *BIR1* expression levels define a threshold beyond which plant immunity is compromised resulting in severe developmental defects and cell death.

Table S1. List of primers used in this study

Description	Forward (5'-3')	Reverse (5'-3')
qRT-PCR:		
TRV	GTGCACGCAACAGTTCTAATCG	GCTGTGCTTTGATTTCTCCACC
TuMV	TGTCGGCTTGGATGGAA	TTAACGTCCTCGGTCGTATGC
BIR1 (AT5G48380)	ATCTCGGATTTTCGGTCTAGC	TCTTGAATACTCGGGAGCAAC
SOBIR (AT2G31880)	CCAAAACCAGGGAAGTTGAA	GTGATCCAACCGCCTAAAGA
BAK1 (AT4G33430)	GACCTTGGGAATGCAAACTCTATC	AAAACCTGATTGGAGTGAAAAGTGAAA
PR4 (AT3G04720)	AGCTTCTTGC GGCAAGTGTTT	TGCTACATCCAAATCCAAGCC
PR1 (AT2G14610)	CGTCTTTGTAGCTCTTGTAGG	TGCCTGGTTGTGAACCCCTTAG
WRKY7 (AT4G24240)	CAAAATGGCTGATATACCATCAGATGA	GCATGGTTGTGGTCTCCTTCG
WRKY29 (AT4G23550)	ATCCAACGGATCAAGAGCTG	GCGTCCGACAACAGATTCTC
PAD3 (AT3G26830)	CAACAACCTCCACTCTTGCTCC	CGACCCATCGCATAAACGTT
ACTIN2 (At3G18780)	GAGAGATTCAGATGCCAGAAAGTC	TGGATTCCAGCAGCTTCCA
CBP20 (AT5G44200)	GTGGCTTTTGTTCGTCCTGTT	GCCCCATTGTCTTCTCTCTTG
PolV transcripts in BIR1 promoter	CGTGATTGACGATATTGATTCTCT	ACTAGAGGTTGTGATTCTGGTTT
PolV transcripts positive control (IGN22)	TGTCCATAGGTTTCGGAATTT	GGCATGGTTTGATATCAGGAG
Chop Experiments		
BIR1 promoter in CHOP qPCR experiments	TTCAGCAAACACCCCAAAAT	TTTCCTTCAGTAGCTTTCTAGTCTTTG
BIR1 promoter in CHOP PCR experiments	CAGATGTACCCGCCAACCCACGGTT	GGTCACGAATGGCGGATTGGCTT
IGN36 in CHOP experiments	GATTTTGATATTGTTACAGCATTGTT	TCCATATTCAGTACTTTTTAACCTACC
At2G36490 in CHOP experiments	ACCGTTTGTATGTAGGGCGAAA	AAGATAACAGAAAAGACGATGATGACG
At1G49490 in CHOP experiments	CCTCGGATCTTTGGAGCATT	TTTCTGGAGCTTTCACATCTGTT
At1G55535 in CHOP experiments	TCCAAGATTGAGCCAAATTA	AAAAGGAGTGGCCAAGTTGGAA
Bisulfite sequencing		
Negative control (At5G48300)	TTTTGAGTTTTGATTTTTTTATGATAATT	ATTACAAATCTCCATAAAAATAATACTT
Bisulfite BIR1 promoter region fragment 1	TATAAAAATTGAATATTATGTTATATATTTAAATAT	ATCTTTATATATAAACACTCTATAATCATCTTA
Bisulfite BIR1 promoter region fragment 2	TAGAGATTTTAATATTATGTAGATTAAGAGTATATT	AAATTTCTACAATTATATTATATAATAAATAATTTAA
M13 primers	GTAACACGACGGCCAGT	AACAGCTATGACCATG
RNA blot probes		
BIR1 AT5G48380	TTCTCTCGCGTTAAGCTA	GAGGCTTACCACACAGATCCA
Gateway Cloning		
attB1adaptBIR1- fragment for the pDONR207	GGGGACAAGTTTGTACAAAAAAGCAGGCTCCTTGGGAGTCATTGCGTTT	
attB2adaptBIR1nostop- fragment for the pDONR207	GGGGACCACTTTGTACAAGAAAGCTGGGTGACGAGCAACTATGAGCTC	
Transgenic overexpression		
OX-BIR1	AATGGATTACAAAGCTATCA	ACTTGATGTTGACGTTGTAG

References

McNellis TW, Mudgett MB, Li K, Aoyama T, Horvath D, Chua NH, Staskawicz BJ. 1998. Glucocorticoid-inducible expression of a bacterial avirulence gene in transgenic Arabidopsis induces hypersensitive cell death. *Plant J* **14**(2): 247-257.

Stroud H, Greenberg MV, Feng S, Bernatavichute YV, Jacobsen SE. 2013. Comprehensive analysis of silencing mutants reveals complex regulation of the Arabidopsis methylome. *Cell* **152**(1-2): 352-364.